

# Europium-Doped Nanocomposite $\text{TiO}_x:\text{SiO}_y$ Layers

Magdalena Zięba,\* Cuma Tyszkiewicz and Paweł Karasiński

*Silesian University of Technology, Department of Optoelectronics, ul. B. Krzywoustego 2, 44-100 Gliwice, Poland*

Received February 7, 2025; accepted March 4, 2025; published March 31, 2025

**Abstract**—The work presents  $\text{TiO}_x:\text{SiO}_y$  nanocomposite layers doped with  $\text{Eu}^{3+}$  ions. Layers were fabricated using the sol-gel method and dip-coating technique. It was shown that the viscosity of sols and the size of optical band gaps increase with increasing concentration of europium ions. Considering the quantum size effect, it was found that the presence of europium ions causes a weakening of the crystallization of titanium oxide. This means that the diameters of scattering centers are smaller, and the layer's surfaces have lower roughness. In this way, the presence of europium ions in  $\text{TiO}_x:\text{SiO}_y$  waveguide layers contributes to reducing optical losses in the latter.

Due to their unique properties, rare earth elements ( $\text{RE}^{3+}$ ) find wide applications in many fields of science and technology. They may be applied to dope materials used in optoelectronics, which gives them new optical properties. Numerous research groups are working on developing active materials for applications in optical amplifiers and lasers. The main problem in the technology of such materials is the selection of the matrix in which the lanthanide ions are bound and a method of introducing them into the matrix. Active materials from which planar waveguides or optical fiber waveguides can be produced are particularly desirable. The research presented here addresses these issues [1–3] and concerns the production of  $\text{Eu}^{3+}$  doped  $\text{TiO}_x:\text{SiO}_y$  nanocomposite layers.

Binary oxide systems are perfect matrices for binding  $\text{RE}^{3+}$  ions.  $\text{RE}^{3+}$ -doped waveguide layers are particularly desirable in optoelectronics. Layers doped with them can be produced from the gas phase using physical (PVD) or chemical (CVD) methods or from the liquid phase using sols prepared by the sol-gel method followed by an appropriate deposition technique [5].

The sol-gel method is a chemical method of producing materials from the liquid phase. Its most significant advantages are the ability to control the structure of the produced material over a wide range and the fact that it does not require complex technological installations. The sol-gel method can be used to produce multicomponent materials with homogeneity at the molecular level and high uniformity of a dopant distribution [6].

As applied to the fabrication of binary oxide systems, the sol-gel offers great potential for controlling their parameters, especially the refractive index and crystallite size, and, in the case of layers, also the surface roughness [4]. Spin-coating and dip-coating techniques are the most

commonly used liquid-phase coating techniques. Still, the dip-coating technique allows for better layer thickness uniformity and can be scaled up to larger substrate surfaces [7–8]. For this reason, the europium-doped  $\text{TiO}_x:\text{SiO}_y$  nanocomposite layers presented here were produced by the dip-coating technique.

In this paper, we present europium-doped  $\text{TiO}_x:\text{SiO}_y$  nanocomposite waveguide layers with a refractive index of  $n \sim 1.65$ , fabricated using the sol-gel method and dip-coating technique. We present the influence of europium doping on the optical properties of the produced layers.

In the studies, tetraethyl orthosilicate ( $\text{Si}(\text{OC}_2\text{H}_5)_4$ ; TEOS) was used as a precursor of silica, titanium (IV) ethoxide ( $\text{Ti}(\text{OC}_2\text{H}_5)_4$ ; TET), as a precursor of titanium oxide, and hexahydrate nitrate (V) europium ( $\text{Eu}(\text{NO}_3)_3 \cdot 6\text{H}_2\text{O}$ ), as a precursor of europium oxide. The solvent used was anhydrous ethanol 99.8% ( $\text{C}_2\text{H}_5\text{OH}$ , EtOH). The hydrolysis and condensation reactions were catalysed by hydrochloric acid (35%). The layers were deposited on soda-lime glass substrates (Menzel Gläser) using the dip-coating technique, and all were annealed at the same temperature of 500°C.

The thicknesses and refractive indices of the produced layers were measured using a SENTECH SE400 monochromatic ellipsometer ( $\lambda = 632.8$  nm). Transmission and reflection spectra were recorded using a spectrophotometer UV-Vis AVANTES AvaSpec-ULS-TEC. A light source AVANTES AvaLight-DH-S-BAL was used to illuminate the structures. Reflection spectra enabled the determination of the optical homogeneity of the layers, while optical forbidden gaps were estimated from the analysis of the absorption edges tails using Tauc method.

For the dip-coating technique, the thicknesses of the produced layers are controlled by the rate  $v$  of withdrawal speed of substrates from a sol. For sols behaving like a Newtonian fluid, the thicknesses  $d$  of the produced layers increase with the increase in the substrate's withdrawal speed  $v$ . The thickness of the layers produced is proportional to  $v^{1/2}$  if the movement of the substrate causes a change in the radius of curvature of the meniscus at the sol-substrate interface [9]. However, if the movement of the substrate does not cause a change in the meniscus, then the layers thicknesses  $d$  is proportional to  $v^{2/3}$  [9]. If layers are fabricated in a wide range of  $v$ , then

\* E-mail: magdalena.zieba@polsl.pl



both the first and the second cases can be distinguished within specific ranges [10]. In practice, linear functions can approximate the experimental dependencies  $d(v)$  with high accuracy. Four such characteristics are presented in Fig. 1. Experimental points are marked with empty diamonds. The dependencies for layers produced from undoped sol (0% mol.  $\text{Eu}^{3+}$ ) are plotted in purple. These layers acted as reference layers. The characteristics  $d(v)$  determined for layers doped with europium in amounts of 1, 3, and 5 mol% are plotted in different colors. In each case, the linear function approximates the experimental data very well. All layers were produced under the same conditions. As seen, along with the increase in europium concentration, the subsequent  $d(v)$  characteristics increase progressively. This results from the increase in sol viscosity as the concentration of europium increases.

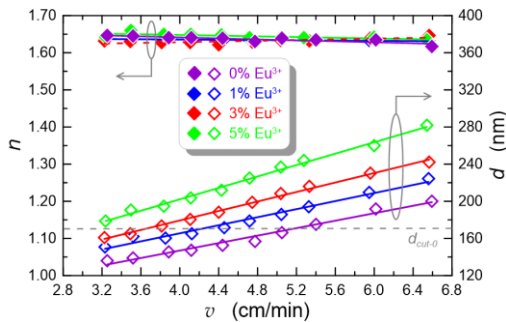


Fig. 1. Influence of substrate withdrawal speed on film thicknesses and refractive indices for  $\text{Eu}^{3+}$  doped  $\text{TiO}_x:\text{SiO}_y$  nanocomposite layers.

The refractive indices of the layers are marked with full diamonds. In this case, the experimental dependencies  $n(v)$  were also approximated by linear functions. As can be seen, the value of the substrate withdrawal speed  $v$  does not affect the value of the refractive index of the layers. The calculated average refractive indices from each relationship and their corresponding standard deviations allow us to conclude that the final refractive index does not depend on  $v$  or the content of europium ions.

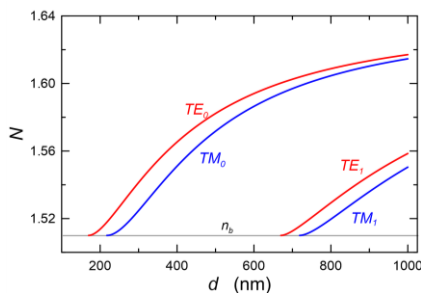


Fig. 2. Modal characteristics of planar waveguide calculated for the refractive index of substrate  $n_b=1.501$ , waveguide layer  $n_1=1.637$ , and cover  $n_c=1.000$ . Wavelength  $\lambda=632.8$  nm.

The average value of the refractive index  $n_1$  calculated from all layers is 1.637. Calculated mode characteristics for such a waveguide layer on a soda-lime substrate with the refractive index of  $n_b=1.510$  are presented in Fig. 2.

The cut-off thickness of the fundamental  $\text{TE}_0$  mode is 170 nm, and that of the  $\text{TE}_1$  mode is 67 nm. In Fig. 1, the thickness level of 170 nm is marked with a horizontal dashed line ( $d_{\text{cut}0}$ ).

The uniformity of optical layers is of great importance in many applications. It is crucial in the case of waveguide layers. Figure 3 shows the transmittance and reflectance of the layers produced at  $v \approx 3.2$  cm/min (Fig. 1). The reflection and transmission characteristics recorded for the soda-lime glass substrate are also plotted. These characteristics are plotted with grey lines.

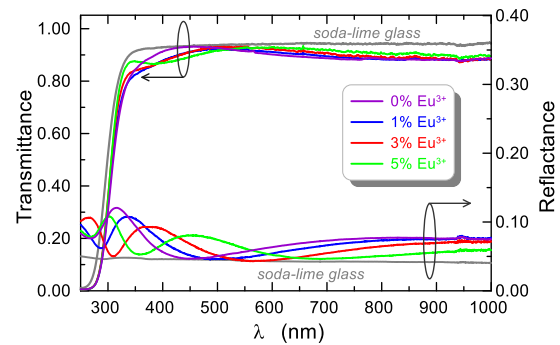


Fig. 3. Transmittance and reflectance of the  $\text{Eu}^{3+}$  doped  $\text{TiO}_x:\text{SiO}_y$  nanocomposite layers.

The graphs show interference minima and maxima. The sharp drop in transmittance below 350 nm results from the absorption edge of the glass substrate occurring in this spectral range. The interference maxima visible in the transmittance characteristics, occurring in the spectral range of 400–600 nm, lie on the transmittance characteristics of the substrate, indicating the optical homogeneity of the layers. Moreover, it can also be seen that the minima of the reflectance characteristics of the layers lie on the reflectance characteristics of the glass substrate, which clearly proves the optical homogeneity of the layers. The position of the interference minimum of the 3% mol  $\text{Eu}^{3+}$  layer in the reflectance characteristic of the substrate glass at a wavelength of 310 nm indicates that at this wavelength no significant light absorption occurs yet in the 3% mol  $\text{Eu}^{3+}$  layer.

From the analysis of the tails of the absorption edge in the transmittance spectra, the widths of the optical band gaps  $E_g$  were determined using the Tauc method. Optical band gaps  $E_g$ , absorption coefficient  $\alpha$  and photon energy  $h\nu$  are connected in Tauc equation:

$$(\alpha h\nu) = B(h\nu - E_g)^\gamma, \quad (1)$$

where  $B$  is a constant, and the factor  $\gamma$  depends on the nature of the electron transition between the edges of valence and the conduction band. Factor  $\gamma$  equals 1/2 or 2 for the direct and indirect allowed transition band gaps, respectively. The method of determining the optical band gaps for a layer 174-nm-thick and containing 3 mol% europium is shown in Fig. 4.

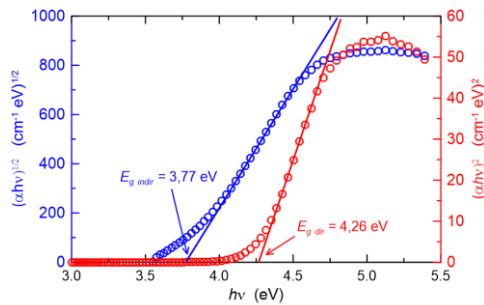


Fig. 4. Normalized absorption coefficients versus photon energy for  $\text{Eu}^{3+}$  doped  $\text{TiO}_x:\text{SiO}_y$  nanocomposite layers (3% mol Eu,  $d=174$  nm).

The influence of the thickness  $d$  of  $\text{Eu}^{3+}$  doped  $\text{TiO}_x:\text{SiO}_y$  nanocomposite layers on the optical band gap widths  $E_g$  is shown in Fig. 5.

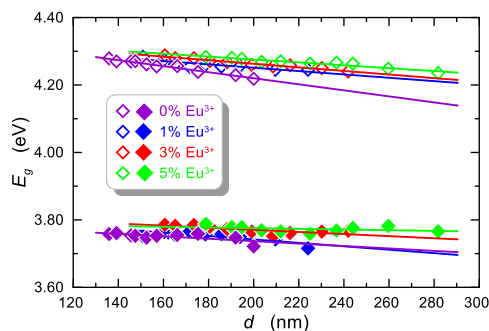


Fig. 5. Influence of the layer thickness of  $\text{Eu}^{3+}$  doped  $\text{TiO}_x:\text{SiO}_y$  nanocomposite layers on optical band gaps.

The increase in europium content contributes to the rise of the optical band gap for both direct and indirect transitions. From the quantum size effect [11], it was estimated that the extreme values of the indirect optical band gap correspond to the diameters  $D$  of the anatase  $\text{TiO}_2$  crystallites, which are 2 and 3 nm, respectively. For the reference layer, larger crystallite diameters were determined. They are 3 and 4 nm, respectively. This means that the presence of  $\text{Eu}^{3+}$  ions stabilizes the amorphous phase of titanium oxide, i.e., weakens its crystallization to the anatase phase. This effect is very beneficial from the point of view of the waveguiding properties of  $\text{TiO}_x:\text{SiO}_y$  nanocomposite layers. This is because the increase in the crystallite diameters results in a simultaneous increase in the roughness  $\sigma$  of the waveguide layer surface. The scattering losses on the crystallites are proportional to  $D^3$ , and those caused by the roughness of the waveguide layer surfaces are proportional to  $\sigma^2$  [10]. Both types of losses are Rayleigh losses, i.e., proportional to  $(-4)$ . It is therefore justified to assume that by doping  $\text{TiO}_x:\text{SiO}_y$  nanocomposite waveguide layers with europium, optical losses can be reduced. This thesis was confirmed by the results of our atomic force microscopy tests of the surface roughness of

waveguide layers, which were not presented here, and by the results of optical loss measurements.

Figure 5 shows the image of  $\text{Eu}^{3+}$  doped  $\text{TiO}_x:\text{SiO}_y$  nanocomposite slab waveguides excited using a prismatic coupler. A streak of scattered light is visible. Furthermore, it can be seen that a significant amount of light reaches the end of the structure.

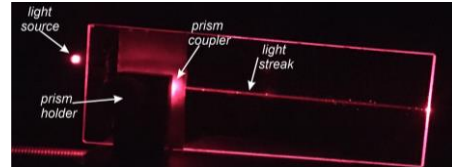


Fig. 5. Picture of the  $\text{Eu}^{3+}$  doped  $\text{TiO}_x:\text{SiO}_y$  waveguided, excited using prism coupler.

In conclusion, two-component waveguide layers  $\text{TiO}_x:\text{SiO}_y$  doped with europium ions  $\text{Eu}^{3+}$  were developed. They were produced using the sol-gel method and dip-coating technique. Spectrophotometric studies of the developed layers showed their optical homogeneity. Optical band gaps were determined using the Tauc method. It was shown that doping with  $\text{Eu}^{3+}$  ions weakens the tendency of  $\text{TiO}_2$  to crystallization, thus stabilizing the amorphous phase and improving the surface smoothness of the  $\text{TiO}_x:\text{SiO}_y$  layers.

This work was financially supported by the project PM-II/SP/0042/2024/02 financed from state budget funds granted by the Polish Minister of Science and Higher Education within the framework of the Polish Metrology II program.

## References

- [1] B. Zheng *et al.*, *Chemical Reviews* **122**, 6, 5519 (2022).
- [2] R.G Manju *et al.*, *RSC Adv.* **10**, 20057 (2020).
- [3] V.P. Prakashan *et al.*, *J. Non.-Cryst. Solids* **482**, 116 (2018).
- [4] X. Chen *et al.*, *Chem. Rev.* **107**, 2891 (2007).
- [5] L.H. Slooff *et al.*, *J. Non.-Cryst. Solids* **296**(3), 158 (2011).
- [6] M. Zięba *et al.*, *Materials* **14**, 7125 (2021).
- [7] P. Karasiński *et al.*, *Thin Solid Films* **519**, 5544 (2011).
- [8] J. Puetz *et al.*, *Dip Coating Technique in: M.A. Aegerter, M. Mennig (Eds) Sol-Gel Technologies for Glass Producers and Users* (Springer, Boston 2004).
- [9] C.J. Brinker, G.W. Scherer, *Sol-Gel Science: The Physics and Chemistry of Sol-Gel Processing* (Wiley & Sons Library: Hoboken, NJ, USA, 2013), pp. 1–908.
- [10] P. Karasiński, M. Zięba, E. Gondek, J. Nizioł, S. Gorantla, K. Rola, A. Bachmatiuk, C. Tyszkiewicz, *Materials* **15**, 7641 (2022).
- [11] P. Karasiński, E. Gondek, S. Drewniak, I.V.J. Kityk, *Sol-Gel Sci. Technol.* **61**, 355 (2012).